Light and depth dependency of nitrogen fixation by the non-photosynthetic, symbiotic cyanobacterium UCYN-A

Mary R. Gradoville [ID],[1*] Ana M. Cabello [ID],[1,2]
Samuel T. Wilson [ID],[3] Kendra A. Turk-Kubo [ID],[1]
David M. Karl [ID],[3] and Jonathan P. Zehr [ID][1]

[1]*Ocean Sciences Department, University of California Santa Cruz, Santa Cruz, CA, USA.*

[2]*Centro Oceanográfico de Málaga, Instituto Español de Oceanografía, Fuengirola, Málaga.*

[3]*Department of Oceanography, University of Hawaii at Manoa, Honolulu, HI, USA.*

Summary

The symbiotic cyanobacterium UCYN-A is one of the most globally abundant marine dinitrogen (N_2)-fixers, but cultures have not been available and its biology and ecology are poorly understood. We used cultivation-independent approaches to investigate how UCYN-A single-cell N_2 fixation rates (NFRs) and *nifH* gene expression vary as a function of depth and photoperiod. Twelve-hour day/night incubations showed that UCYN-A only fixed N_2 during the day. Experiments conducted using *in situ* arrays showed a light-dependence of NFRs by the UCYN-A symbiosis, with the highest rates in surface waters (5–45 m) and lower rates at depth ($\geq$ 75 m). Analysis of NFRs versus *in situ* light intensity yielded a light saturation parameter (I_k) for UCYN-A of 44 μmol quanta m^{-2} s^{-1}. This is low compared with other marine diazotrophs, suggesting an ecological advantage for the UCYN-A symbiosis under low-light conditions. In contrast to cell-specific NFRs, *nifH* gene-specific expression levels did not vary with depth, indicating that light regulates N_2 fixation by UCYN-A through processes other than transcription, likely including host–symbiont interactions. These results offer new insights into the physiology of the UCYN-A symbiosis in the subtropical North Pacific Ocean and provide clues to the environmental drivers of its global distributions.

Introduction

Phytoplankton production in most ocean ecosystems is limited by the availability of nitrogen (N) (Moore *et al*., 2013). Biological dinitrogen (N_2) fixation, the reduction of N_2 into ammonia, supplies approximately half of Earth's reactive N (Galloway *et al*., 2004) and supports a large fraction of new production and export in the N-limited subtropical gyres (Karl *et al*., 1997). The process of N_2 fixation is carried out by some Bacteria and Archaea, termed diazotrophs. In the oceans, most N_2 fixation is likely performed by cyanobacteria, including the filamentous cyanobacteria *Trichodesmium*, heterocyst-forming symbionts of diatoms (*Richelia* and *Calothrix*), unicellular symbionts of haptophytes (UCYN-A), and other unicellular groups (*Crocosphaera* and *Cyanothece*-like organisms). These cyanobacterial diazotrophs differ greatly in their physiology, biogeography, and ecology (Zehr and Capone, 2020). Understanding the different responses of diazotroph taxa to factors such as temperature, light, and nutrients is important for parameterizing prognostic ocean models (Wang *et al*., 2019). However, despite the importance of the globally abundant but uncultivated diazotroph, UCYN-A, to marine N_2 fixation (Martínez-Pérez *et al*., 2016), the environmental factors controlling its growth and N_2 fixation rates (NFRs) are poorly understood.

UCYN-A is a unicellular cyanobacterium living in a unique symbiosis with a haptophyte alga (Zehr *et al*., 2016). The genome of UCYN-A is streamlined, lacking genes for photosystem II, carbon fixation, and the TCA cycle (Zehr *et al*., 2008; Tripp *et al*., 2010). Incapable of oxygenic photosynthesis or carbon fixation, UCYN-A relies on its algal host for fixed carbon, which it receives in exchange for fixed N (Thompson *et al*., 2012). Recent cultivation-independent experiments indicate that the temperature and nutrient controls for the UCYN-A symbiosis may diverge from those of other cyanobacterial diazotrophs. For instance, UCYN-A fixes N_2 in the Arctic Ocean at temperatures below the thermal limits of other cyanobacterial diazotrophs (Harding *et al*., 2018). Additionally, N_2 fixation by UCYN-A does not appear to be inhibited by the presence of fixed N (nitrate and ammonium; Krupke *et al*., 2015; Mills

et al., 2020), despite the high energetic cost of N_2 fixation relative to fixed N uptake (Falkowski, 1983).

Light is another primary ecological control for marine diazotrophs (Luo *et al*., 2014). All known photosynthetic diazotrophic cyanobacteria depend on light, but individual taxa display different light affinities (Villareal, 1990; Breitbarth *et al*., 2008; Foster *et al*., 2010; Garcia *et al*., 2013), allowing them to inhabit different depths within the euphotic zone (Tang and Cassar, 2019). While UCYN-A does not possess the light-harvesting photosystem II apparatus and thus does not photosynthesize, a light dependency for N_2 fixation by UCYN-A is expected, because: (i) UCYN-A depends on fixed carbon from its photosynthetically active host (Zehr *et al*., 2008; Thompson *et al*., 2012) and (ii) UCYN-A may use light-driven photosystem I reactions to help fuel N_2 fixation. Still, the effects of light intensity on the UCYN-A symbiosis are unknown.

In addition to providing the energy for N_2 fixation by cyanobacteria, light also exerts an indirect control over the operation of nitrogenase due to the extreme sensitivity of this enzyme to oxygen (Gallon, 1992). Diazotrophic cyanobacteria use different strategies to protect nitrogenase from the oxygen produced during photosynthesis. Some filamentous cyanobacteria perform both photosynthesis and N_2 fixation during the day but spatially segregate the two processes by only performing N_2 fixation in specialized heterocyst cells (Villareal, 1992). In contrast, unicellular cyanobacteria, such as *Crocosphaera*, temporally separate N_2 fixation and oxygen evolution by fixing carbon during the day and N_2 at night (Mitsui *et al*., 1986; Tuit *et al*., 2004). Since UCYN-A does not produce oxygen (Zehr *et al*., 2008), its daily pattern of N_2 fixation may be expected to diverge from those of other unicellular cyanobacterial diazotrophs. Indeed, indirect evidence, including single-cell rate measurements and daily transcriptional patterns of the *nifH* gene (encoding for the iron protein of nitrogenase), suggest that UCYN-A fixes N_2 during the day (Church *et al*., 2005b; Krupke *et al*., 2013; Thompson *et al*., 2014; del Carmen Muñoz-Marin *et al*., 2019), likely facilitated by hopanoid membrane lipids restricting the diffusion of oxygen to nitrogenase (Cornejo-Castillo and Zehr, 2019). However, absolute rates of N_2 fixation for the day versus night by UCYN-A have not been demonstrated.

Here, we investigate the effects of light on N_2 fixation by the UCYN-A symbiosis. We present results from $^{15}N_2$ incubations paired with single-cell analyses to compare daytime and nighttime UCYN-A NFRs and to test how rates vary with depth and *in situ* light intensity. We also compare the depth-dependence and diurnal pattern of UCYN-A NFRs to patterns in expression levels of the *nifH* gene. Our results offer new insights into the

environmental drivers of N_2 fixation in the subtropical oceans and the physiological regulation of N_2 fixation by this uncultivated marine diazotroph.

Results

Oceanographic conditions

Experiments were conducted using samples collected from the centre of a cyclonic eddy and an anticyclonic eddy near Station ALOHA (A Long-term Oligotrophic Habitat Assessment) in the North Pacific Subtropical Gyre (NPSG; Fig. 1). Lagrangian sampling within eddies was conducted in order to examine diurnal changes in *nifH* gene expression with depth while minimizing spatial effects. Sampling eddies of opposite polarity also provided the opportunity to evaluate differences in UCYN-A cell-specific NFRs resulting from varying nutrient conditions caused by the uplift or depression of isopycnals.

In the lower euphotic zone, concentrations of nitrate +nitrite (N + N), soluble reactive phosphorus (SRP), and chloropigments were higher in the cyclone than in the anticyclone (SRP = 2.27 and 0.23 μmol L^{-1} at 150 m, respectively, Fig. S1), indicative of eddy-induced isopycnal uplift (McGillicuddy and Robinson, 1997; Barone *et al*., 2019). However, concentrations of N + N and SRP were low ($\leq$ 0.04 and $\leq$ 0.05 μmol L^{-1},
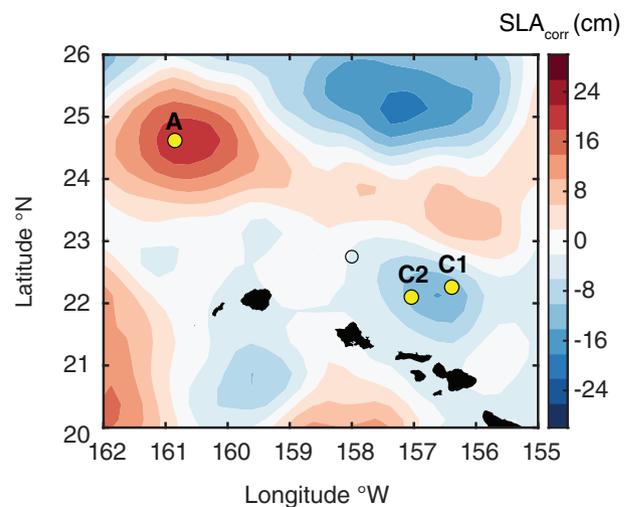
Fig. 1. Sampling locations superimposed onto a corrected satellite Sea Level Anomaly (SLA$_{corr}$) field for April 3, 2018. Station A: anticyclone array, Day 2, and Night 2 experiments. Station C1: cyclone array 1 and diel nucleic acid sampling experiments. Station C2: cyclone array 2, Day 1, and Night 1 experiments. Exact locations of all experiments are provided in Table S1. The open circle shows the location of Station ALOHA. Sea level anomaly data were retrieved from the Copernicus Marine and Environment Monitoring Service (http://www.marine.copernicus.eu) and corrected for an interannual linear trend and the seasonal cycle, following Barone *et al*. (2019).

respectively) within the top 75 m of the cyclone and the top 100 m of the anticyclone where UCYN-A NFRs were measured (Fig. S1). Sea surface temperatures were slightly lower in the anticyclone (22.9°C) than in the cyclone (23.4–23.5°C); temperatures in the *in situ* array samples used for single-cell NFR measurements ranged from 22.4 to 23.5°C. Daily integrated Photosynthetically Active Radiation (PAR) was lower during sampling of the anticyclone than the cyclone (21.4 and 47.4–48.8 mol quanta m^{-2} d^{-1}, respectively) due to cloud cover. Sampling locations and ancillary data from each of our experiments are presented in Table S1; these values were within the typical ranges reported at Station ALOHA in springtime (Letelier *et al*., 1996, https://hahana.soest. hawaii.edu/hot/hot-dogs/).

Community NFRs and diazotrophic abundances

Community NFRs were measured via 24-h $^{15}N_2$ incubations conducted using free-floating, *in situ* arrays (Williams *et al*., 2004; Böttjer *et al*., 2017). Surface NFRs (4.9–9.1 nmol N l^{-1} d^{-1} at 5 m) were within the range of rates previously observed at Station ALOHA [~0.2–19.5 nmol N l^{-1} d^{-1} at 5 m, (Böttjer *et al*., 2017)]. Rates decreased with depth and were higher in the anticyclone than in the cyclone, consistent with previous observations in the NPSG (Fong *et al*., 2008; Church *et al*., 2009; Böttjer *et al*., 2017, Table S2). The UCYN-A1 symbiosis was likely the most abundant diazotroph quantified, given that *nifH* gene abundances at 5 m (2.8–6.2 × 10^5 *nifH* copies l^{-1}) were ≥ 40-times higher than those of any other group (Table S2). UCYN-A1 *nifH* gene abundances decreased with depth in all three arrays.

Community NFRs from 25 m samples were also measured using 12-h deck-board incubation experiments conducted during the day and night periods. Rates ranged from 2.2 to 2.5 nmol N l^{-1} d^{-1} during the day and from BD to 0.7 nmol N l^{-1} d^{-1} at night (Table S2). The UCYN-A1 symbiosis was likely the most abundant diazotroph in all experiments (up to 7.1 × 10^5 *nifH* copies l^{-1}), with *nifH* gene abundances ≥ 35-times greater than those of any other quantified diazotroph (Table S2). Abundances of the nighttime-fixing diazotrophs *Crocosphaera* and *Cyanothece* were lower in the Night 2 experiment than the Night 1 experiment (Table S2), which may explain the lack of detectable nighttime NFRs during Night 2.

UCYN-A cell-specific NFRs

Cell-specific NFRs of UCYN-A symbioses were measured by subsampling from $^{15}N_2$ incubations, visualizing UCYN-A symbioses using a double catalysed reporter deposition fluorescence *in situ* hybridization (CARD-FISH) assay, and measuring the size and N isotopic composition of UCYN-A symbioses using nanoscale secondary ion mass spectrometry (nanoSIMS). Because a large fraction of fixed N is transferred from UCYN-A to the haptophyte host during a 24-h incubation (Thompson *et al*., 2012), the symbiont and host cells were analysed together and all rates are presented per UCYN-A/ haptophyte association (Fig. S2). All experiments targeted UCYN-A1, the UCYN-A sublineage with the smallest cell size (symbiosis diameter ~ 1–3 μm) and the highest abundances in the NPSG (Thompson *et al*., 2012; Turk-Kubo *et al*., 2017).

Cell-specific NFRs from daytime and nighttime $^{15}N_2$ incubations indicate that UCYN-A primarily fixed N_2 during the day (Fig. 2). Mean rates in daytime experiments were 4.6–5.3 fmol N $cell^{-1}$ day^{-1}, while rates in the nighttime experiments were very low (0.16 fmol N $cell^{-1}$ $night^{-1}$, Night 1) or below detection limits (Night 2). The low but detectable rate observed during Night 1 represents ~3.5% of total daily N_2 fixation by UCYN-A.

UCYN-A cell-specific NFRs decreased with depth in all three *in situ* array experiments (Fig. 3). There was no significant difference in cell-specific rates among 5, 25, and 45 m samples [two-way ANOVA, Tukey Honest Significant Difference (HSD) $P > 0.05$]; however, rates were significantly (~1.7-times) lower at 75 m than in the upper three depths (two-way ANOVA, Tukey HSD $P < 0.0001$). Rates at 100 m, available only for the anticyclone array, were ~ 16-times lower than rates at 5, 25, or 45 m (one-way ANOVA, Tukey HSD $P < 0.000001$) and ~ seven-times lower than rates at 75 m (one-way ANOVA, Tukey HSD $P = 0.047$). There was no significant difference between cell-specific rates in the cyclonic and anticyclonic eddies (two-way ANOVA, $P > 0.05$).

Analysis of UCYN-A cell-specific NFRs as a function of *in situ* light intensity resembles a typical photosynthesis-
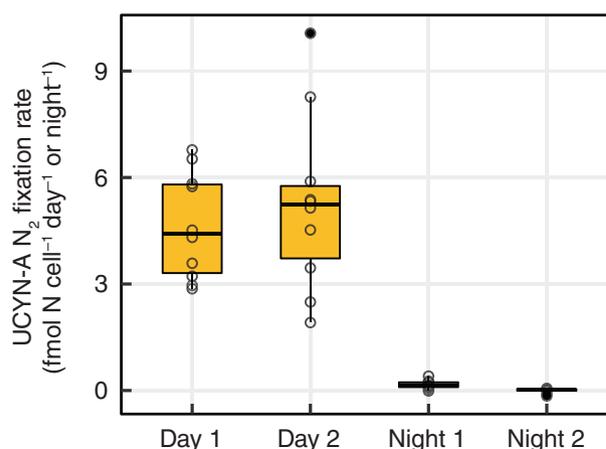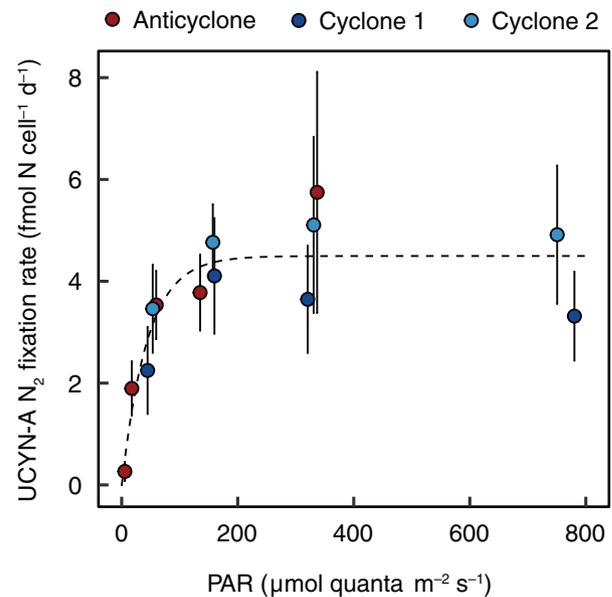
Fig. 2. UCYN-A1 cell-specific NFRs measured using 12-h deck-board incubations during the day and night periods. Each circle represents the rate measured from an individual UCYN-A1 association. Boxplots represent summary statistics; black points represent outliers.

Anticyclone   Cyclone 1   Cyclone 2

UCYN-A N$_2$ fixation rate (fmol N cell^{-1} day^{-1})
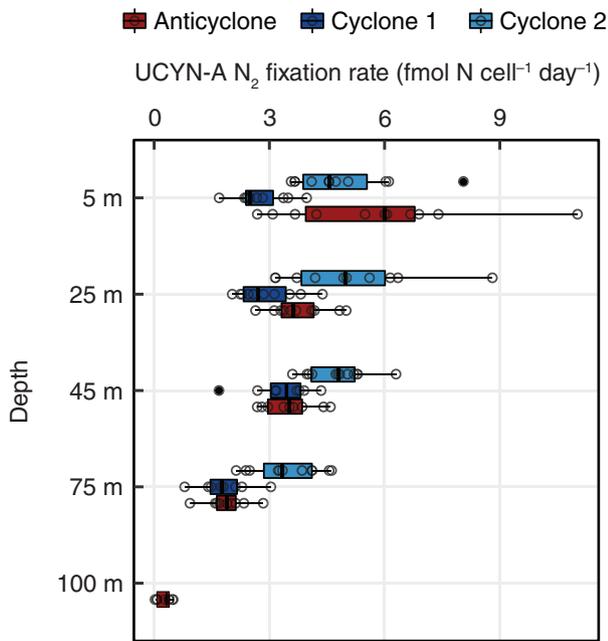
Fig. 3. UCYN-A1 cell-specific NFRs measured over 24-h using free-floating *in situ* arrays deployed in anticyclonic (red) and cyclonic (blue) eddies. Each circle represents the rate measured from an individual UCYN-A1 association. Boxplots represent summary statistics; black points represent outliers.

Fig. 4. UCYN-A1 cell-specific NFR as a function of average daily *in situ* light intensity. Symbols and error bars represent mean and standard deviation ($n = 8$–12 symbioses analysed per sample). The dashed line represents the fitted light response curve, using the model of Webb *et al.* (1974). Parameters for the light curve are presented in Table 1.

versus-irradiance or NFR-versus-irradiance curve (Fig. 4). Light response curves were fit for UCYN-A cell-specific rates and for NFRs of cultured cyanobacterial diazotrophs from previous laboratory studies, using the model of Webb *et al.* (1974). The I_k of UCYN-A (44 μmol quanta m^{-2} s^{-1}) was lower than those of other cyanobacterial diazotrophs, both for curves constructed using the average PAR from daylight hours (Table 1, Fig. S3) and using daily integrated PAR (available for *Crocosphaera* only for comparison, Fig. S4). Using the Beer–Lambert law with values for the climatological average surface PAR and light attenuation coefficient at Station ALOHA from Letelier *et al.* (2004), the daily integrated PAR I_k value for UCYN-A (1.97 mol quanta m^{-2} day^{-1}) corresponds to average depths of 88 m and 61 m for summer and winter, respectively.

The contribution of UCYN-A to community NFRs at each station and depth was estimated by multiplying UCYN-A *nifH* gene abundances by cell-specific NFRs and dividing by community (bulk) NFRs (Table S3). Contribution estimates for *in situ* array experiments ranged from $13 \pm 104\%$ to $52 \pm 35\%$ and increased with depth. These estimates should be viewed with caution, as (i) *nifH* gene abundances may under- or over-estimate cell concentration due to incomplete DNA extraction efficiency and/or polyploidy (Boström *et al.*, 2004; Sargent *et al.*, 2016) and (ii) the contribution of UCYN-A may be underestimated for a number of reasons (see Experimental procedures), including

dilution of the heavy isotope through the CARD-FISH procedure (Musat *et al.*, 2014; Stryhanyuk *et al.*, 2018; Meyer *et al.*, 2020) and/or if fixed N is rapidly transferred to other organisms or to dissolved N pools. Applying the correction factor suggested by Meyer *et al.* (2020) to account for the dilution of ^{15}N through CARD-FISH [maximum dilution factor $= 75\%$, Meyer *et al.* (2020)] raises the maximum possible contributions of UCYN-A to community NFRs in *in situ* array experiments to 53–211% (Table S3).

UCYN-A nifH *gene expression patterns*

UCYN-A *nifH* gene expression levels were measured via Lagrangian sampling through the diel cycle using seawater samples collected from 5, 75, and 100 m within the cyclonic eddy. Abundances of *nifH* genes and transcripts decreased with depth (Fig. S5). The normalized *nifH* expression (UCYN-A *nifH* transcripts gene copy^{-1}) followed a diel cycle, with highest expression in the early morning and lowest expression in evening and night (Fig. 5). There was no significant difference in normalized *nifH* expression among depths (two-way ANOVA, Tukey HSD $P > 0.05$).

Discussion

UCYN-A fixes nitrogen during the day

UCYN-A is unique among the known marine cyanobacterial diazotrophs in terms of its streamlined

Table 1. Light response curve parameters for UCYN-A cell-specific N_2 fixation rates (NFRs), as well as for four cultured cyanobacterial diazotrophs using values from the literature. All curves were fit using the model of Webb *et al.* (1974). Values for α, NFR_{max} and NFR_0 represent parameter estimates ± standard error; I_k values represent estimates ± propagated standard error.

	α[a]	NFR_{max}[b]	NFR_0[c]	I_k[d]	NFR method	NFR unit	Reference
UCYN-A	0.010 ± 0.05	4.52 ± 0.85	-0.02 ± 0.85	44 ± 23	$^{15}N_2$	fmol N cell⁻¹ day⁻¹	This study
Trichodesmium	0.0042 ± 0.002	2.97 ± 1.04	1.16 ± 0.25	706 ± 415	ARA[e] (4:1 ratio[f])	mol N mol chl a^{-1} h⁻¹	Breitbarth *et al.* (2008)
Crocosphaera	0.25 ± 0.04	20.7 ± 0.70	-3.14 ± 0.90	83 ± 13	ARA (3:1 ratio)	fmol N cell⁻¹ h⁻¹	Garcia *et al.* (2013)
Richelia	$8.80 \times 10^{-5} \pm 4.21 \times 10^{-5}$	$8.11 \times 10^{-3} \pm 1.18 \times 10^{-3}$	$1.41 \times 10^{-3} \pm 1.07 \times 10^{-3}$	92 ± 46	ARA	nM ethylene trichome⁻¹ h⁻¹	Villareal (1990)
Calothrix	0.012 ± 0.004	2.76 ± 0.30	1.02 ± 0.027	225 ± 72	ARA	μmol C_2H_4 mg chl a^{-1} h⁻¹	Foster *et al.* (2010)

[a] α: light affinity coefficient; units are the NFR unit per μmol quanta m⁻² s⁻¹.
[b] NFR_{max}: maximum NFR.
[c] NFR_0: dark NFR.
[d] I_k: light saturation parameter (μmol quanta m⁻² s⁻¹).
[e] Acetylene reduction assay.
[f] Assumed molar ratio of ethylene production to N_2 fixation.

genome and metabolism, symbiotic relationship with a haptophyte alga, and activity in high-latitude oceans (Tripp *et al.*, 2010; Thompson *et al.*, 2012; Harding *et al.*, 2018). We show that UCYN-A also has a unique diel pattern in N_2 fixation: unlike other unicellular cyanobacterial diazotrophs, UCYN-A largely fixes N_2 during the day and not at night (Fig. 2). Nighttime NFRs require greater temporal resolution, as it remains an open question whether the low but detectable rate observed during the Night 1 experiment reflects NFRs restricted to 1–2 h post-dusk or pre-dawn rather than a low sustained rate during the entire night period. Regardless, we found that the vast majority (> 96%) of daily N_2 fixation occurs during the day.

Our results agree with other less direct evidence that UCYN-A fixes N_2 primarily during the day rather than at night. UCYN-A has maximum *nifH* gene expression levels during the morning (Church *et al.*, 2005b; Thompson *et al.*, 2014), and the daily transcriptional pattern of UCYN-A is similar to those of other daytime N_2-fixers such as *Trichodesmium* (del Carmen Muñoz-Marin *et al.*, 2019). Additionally, a previous nanoSIMS-based study by Krupke *et al.* (2013) reported no difference in the ^{15}N atom% enrichment of UCYN-A cells incubated in the day only versus the day and night, which implies N_2 fixation restricted to the day but could have been confounded by fixed N release at night. The present results verify that the vast majority (> 96%) of daily net N_2 fixation by the UCYN-A symbiosis occurs during the day.

The apparent contradiction of daytime N_2 fixation by a unicellular cyanobacterium is less surprising when considering that UCYN-A lacks genes for the oxygen-evolving photosystem II apparatus (Zehr *et al.*, 2008). However, while UCYN-A does not produce oxygen, its nitrogenase enzymes are still vulnerable to inactivation by oxygen produced by its photosynthetic haptophyte host, as well as by oxygen in the surrounding seawater. It is unknown how UCYN-A NFRs vary over the day period, and whether the timing of maximum N_2 fixation and host carbon fixation rates are temporally decoupled as they may be for *Trichodesmium* (Chen *et al.*, 1999; Berman-Frank *et al.*, 2001). Oxygen consumption processes by UCYN-A (respiration and the Mehler reaction) likely play a major role in preventing the oxygen inactivation of nitrogenase (Gallon, 1992; Milligan *et al.*, 2007). Finally, the UCYN-A genome contains genes encoding hopanoid membrane lipids, which may restrict oxygen diffusion and help to protect nitrogenase from oxygen in UCYN-A and other non-heterocyst-forming cyanobacterial diazotrophs (Cornejo-Castillo and Zehr, 2019).

Cell-specific rates vary with depth and light intensity

Cell-specific NFRs by the UCYN-A symbiosis decrease with depth in the water column (Fig. 3). This depth-
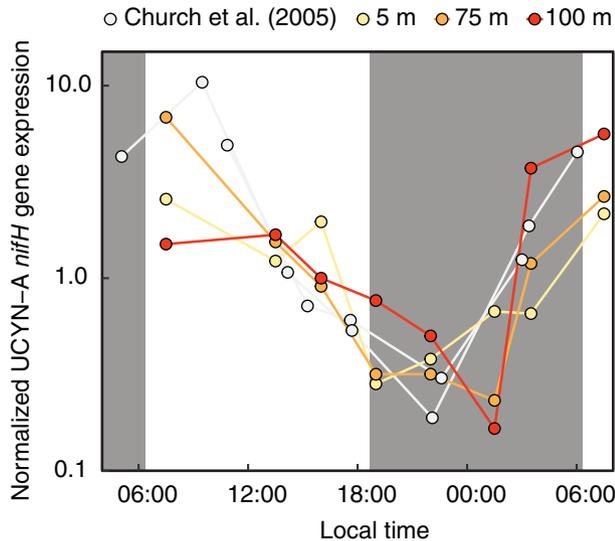
Fig. 5. UCYN-A1 *nifH* gene expression pattern measured at three depths over a 24-h time course. The mean *nifH* transcripts gene copy^{-1} at each time-point were normalized to the median transcripts gene copy^{-1} at each depth from the full time-series, as in Thompson *et al.* (2014). Previous measurements by Church *et al.* (2005b) at Station ALOHA (25 m depth) using the same normalization method are plotted for comparison. Shaded areas represent times of darkness.

dependence appears to be driven by light: similar NFRs were observed under similar light intensities despite differences in sampling depth and station (Fig. 4), and there were minimal changes in other abiotic factors (temperature and nutrients) with depth (Table S1, Fig. S1). Two mechanisms likely drive the light-dependence of N_2 fixation by UCYN-A. First, light limitation likely reduces rates of photosynthesis and carbon fixation by the haptophyte host. While carbon fixation rates are not available in the present study, Martínez-Pérez *et al.* (2016) previously observed a linear correlation between host carbon fixation rates and NFRs within the UCYN-A symbiosis. Second, under light-limiting conditions, UCYN-A likely produces less reducing power or ATP through the light-driven photosystem I complex (Zehr *et al.*, 2008; Cornejo-Castillo *et al.*, 2016). Thus, we expect that the energy available for N_2 fixation by UCYN-A is linked to light directly through light-driven photosystem I reactions and also indirectly through photosynthate transfer from the host.

Our UCYN-A light response curve (Fig. 4) can be compared with the light responses of other cyanobacterial marine diazotrophs. The N_2 fixation assay method ($^{15}N_2$ fixation vs. acetylene reduction) and biomass metric used for normalization differ among individual studies, making it difficult to compare the light affinity coefficient (α); however, the light saturation parameter (I_k), which reflects the irradiance at which the onset of light saturation occurs, is an intercomparable metric when using the same NFR-

versus-irradiance model (Staal *et al.*, 2002). We fit light response curves using available data from several cultured cyanobacterial diazotroph isolates (Villareal, 1990; Breitbarth *et al.*, 2008; Foster *et al.*, 2010; Garcia *et al.*, 2013, Table 1, Figs. S3 and S4), and found that the I_k value for UCYN-A was considerably lower than those for other taxa. This may be at least partially driven by photosynthetic characteristics of the haptophyte host. Studies using *Emiliania huxleyi* and *Isochrysis galbana*, two model haptophyte species, show that these organisms often display high saturating irradiance compared with other eukaryotic algae (Richardson *et al.*, 1983; Zondervan, 2007; Yang *et al.*, 2020). The UCYN-A1 host is known to be a haptophyte closely related to *Braarudosphaera bigelowii* (Thompson *et al.*, 2012), but its exact taxonomic identity and photosynthetic characteristics have not been determined. Unfortunately, single-cell ^{13}C fixation rates are not available for the present study, so the I_k value for N_2 fixation by UCYN-A and carbon fixation by the haptophyte host cannot be compared. The photosynthetic light affinity of the UCYN-A host should be further explored.

The low I_k value we observed suggests that UCYN-A is particularly well suited for N_2 fixation at low light intensities and may help explain its unique biogeography. While the distributions of most cyanobacterial diazotrophs are largely limited to the subtropical and tropical oceans, where solar radiation is high, UCYN-A has been observed in temperate and high-latitude environments, where solar radiation is lower through most of the year (Gradoville *et al.*, 2017; Shiozaki *et al.*, 2017; Harding *et al.*, 2018; Tang and Cassar, 2019; Cheung *et al.*, 2020; Raes *et al.*, 2020). Additionally, maximal UCYN-A abundances are often located deeper in the water column than maximal abundances of other diazotrophs, including *Trichodesmium*, *Crocosphaera,* and *Richelia/Calothrix* (Moisander *et al.*, 2010; Tang and Cassar, 2019). At Station ALOHA, the majority of bulk N_2 fixation occurs in the upper 45 m (Böttjer *et al.*, 2017), but our observed I_k for UCYN-A corresponds to average depths of 88 m and 61 m in the summer and winter, respectively, suggesting that maximal NFRs by UCYN-A may extend deeper in the water column than those of other dominant marine diazotrophs. Indeed, our estimates of UCYN-A contribution to bulk N_2 fixation increased with depth (Table S3), suggesting an important role of UCYN-A in driving N_2 fixation in the lower euphotic zone of the NPSG. A low I_k may help UCYN-A thrive in the high latitude oceans and at depths within the lower euphotic zone where light levels could be prohibitively limiting for other cyanobacterial diazotrophs.

The light response curves from our study were generated *in situ*: samples were collected from a series of depths and incubated at the depth from which they were

collected. Light response curves are more routinely generated *in vitro* by subjecting a culture or seawater sample to a controlled light gradient while holding other abiotic parameters constant. There is precedent for *in situ* light response curves (Forget *et al*., 2007; Li *et al*., 2011; Kovač *et al*., 2016b) and photosynthesis-versus-irradiance curve parameters can be similar using *in vitro* and *in situ* methods (Forget *et al*., 2007). Still, there are noteworthy differences between our study and the *in vitro* studies used (Villareal, 1990; Breitbarth *et al*., 2008; Foster *et al*., 2010; Garcia *et al*., 2013), so comparisons should be viewed with caution. While light was the primary factor changing with depth, there were also small changes in temperature among our samples (range: 22.4–23.5°C, Table S1). Additionally, our experiments sampled different populations of UCYN-A. The deep, light-limited UCYN-A populations were always located below the mixed layer (75 and 100 m samples, Table S1) and thus were likely acclimated to low-light conditions. Because light was saturating at the surface, our derived I_k likely reflects the light response of these deeper populations. Finally, while *in vitro* studies use constant light intensity of the same spectral quality in all treatments, our samples experienced the natural sinusoidal light cycle and ambient spectral quality, with presumably blue-enriched light at depth (Kovač *et al*., 2016a). Our estimate of the NFR_{max} parameter for UCYN-A may thus be more analogous to P^B_{opt} (maximum rate within a water column) than P^B_{max} (maximum rate in short incubations under constant irradiance) (Behrenfeld and Falkowski, 1997), and consequently, our I_k estimate may reflect ecological gradients as well as the physiological characteristics of UCYN-A. The NFR-versus-irradiance relationship for UCYN-A should be further explored to disentangle the possibly confounding effects of temperature, light acclimation, and spectral quality.

nifH *gene expression does not decrease with depth*

The expression of *nifH* genes by cyanobacterial diazotrophs is strongly regulated over the diel cycle, allowing the production of nitrogenase to be optimally synced with timing of N₂ fixation (Wyman *et al*., 1996; Wilson *et al*., 2017). The diel pattern of *nifH* gene expression (transcripts gene copy⁻¹) we observed, with the highest expression in the morning and lowest expression in the evening, is consistent with previous studies of UCYN-A in surface waters (Church *et al*., 2005b; Thompson *et al*., 2014; del Carmen Muñoz-Marin *et al*., 2019). However, comparing expression levels among depths shows no apparent regulation of *nifH* gene expression with depth or light intensity (Fig. 5). This is surprising, since the amplitude of the expression of most genes with diel patterns diminishes below the mixed layer (Vislova

et al., 2019) and because there has been some evidence that *nifH* gene expression levels are linked to NFRs (e.g., Zehr *et al*., 2007), which varied strongly with depth in our experiments (Fig. 3). Our finding of a depth- and light-dependence for cell-specific NFRs but not for gene-specific *nifH* expression shows that light intensity controls N₂ fixation in UCYN-A through processes other than transcription. It is possible that levels of *nifH* mRNA translation are upregulated or downregulated to modulate the reaction efficiency given ambient light and oxygen levels. Light may also control N₂ fixation by regulating the enzymatic activity of nitrogenase, including via post-translational regulation. In *Trichodesmium*, light intensity affects NFRs but not NifH protein levels (Kranz *et al*., 2010; Levitan *et al*., 2010), apparently due to post-translational modification of the iron protein of nitrogenase, which alternates between a high molecular mass, active form and a low molecular mass, inactive form over the diel cycle (Ohki *et al*., 1992; Zehr *et al*., 1993). It is also likely that the light-dependence of NFRs reflects the photosynthesis-versus-irradiance relationship of the host, which may impact the amount of organic carbon available for the symbiont and consequently affect levels of NifH protein synthesis and/or nitrogenase activity. Further work is needed to elucidate the mechanisms through which light controls N₂ fixation by the UCYN-A symbiosis.

Finally, these results highlight the difficulty in using transcriptional activity to predict microbial rates. *nifH* gene expression levels are commonly used as a proxy for taxa-specific nitrogenase activity and/or NFRs (e.g. Goebel *et al*., 2008; Jayakumar *et al*., 2012; Turk-Kubo *et al*., 2012). However, the lack of correspondence between *nifH* gene-specific expression levels and cell-specific NFRs we observed shows that measuring *nifH* gene expression alone would not capture the response of UCYN-A to the water column light gradient. Since the relationship between *nifH* gene transcription and NFRs is not fully understood, attempts to use *nifH* gene expression to predict rates should be viewed with caution.

Conclusions

We show that N₂ fixation by UCYN-A is strongly linked to light, both through the diel light cycle and through the vertical gradient of light with depth. Over the diel cycle, *nifH* gene expression and cell-specific NFRs were associated with the light period, with the highest *nifH* expression in the early morning and the vast majority of N₂ fixation taking place during the day. Over vertical space, UCYN-A NFRs varied strongly with depth and *in situ* light intensity, despite the fact that UCYN-A is not photosynthetic. The NFR-versus-irradiance relationship we observed indicates that UCYN-A may have an ecological advantage over other cyanobacterial diazotrophs under low-light

conditions, information which may be useful in parameterizing NFRs in global ocean models. Finally, our finding that *nifH* gene-specific expression did not decrease with depth or *in situ* light intensity implies that light intensity controls NFRs through a process other than transcription and highlights the challenges in using gene expression as a proxy for microbial activity rates. Until UCYN-A is established in culture, more field-based experiments targeting individual cells will be critical to unravelling the many mysteries concerning the physiology and ecology of this globally abundant marine diazotroph.

Experimental procedures

Sample collection and experimental design

Samples were collected during the Hawaiian Eddy Experiment cruise aboard the R/V Falkor from 27 March to 10 April 2018. This expedition sampled two mesoscale eddies (one cyclone and one anticyclone) near Station ALOHA in the NPSG (Fig. 1). Three sets of experiments were conducted to test the effects of depth/light and photoperiod on N_2 fixation by UCYN-A: (i) 24-h *in situ* array experiments, (ii) 12-h deck-board incubations, and (iii) diel nucleic acid sampling. The *in situ* array and deck-board incubation experiments were conducted within the cyclonic and anticyclonic eddies, while the diel sampling was conducted only within the cyclonic eddy (Fig. 1).

The effects of depth and light on UCYN-A cell-specific NFRs were tested via $^{15}N_2$ tracer experiments conducted using *in situ* arrays. Seawater was collected pre-dawn from depths of 5, 25, 45, 75, 100, and 125 m using Niskin® sampling bottles attached to a rosette equipped with a conductivity–temperature–depth (CTD) package. Seawater was sub-sampled into 4.3 l acid-washed, MilliQ-rinsed polycarbonate bottles for $^{15}N_2$ incubations, T_{zero} $\delta^{15}PN$ natural abundance measurements, and DNA collection. Incubation bottles were subsequently spiked with $^{15}N_2$ (see below) and attached to a free-drifting array where they were incubated for 24 h at the depths from which they had been collected, thus experiencing *in situ* light and temperature conditions. Arrays were recovered after 24 h and incubation bottles were subsampled for CARD-FISH and nanoSIMS (see below).

The effect of photoperiod on UCYN-A cell-specific NFRs was tested via deck-board $^{15}N_2$ incubation experiments. Seawater was collected from 25 m as described above from CTD casts prior to either dawn (Day 1 and Day 2 incubations, running from approximately sunrise to sunset) or dusk (Night 1 and Night 2 incubations, running from approximately sunset to sunrise). Incubation bottles were spiked with $^{15}N_2$ (see below) and incubated in deck-board, surface seawater-cooled incubators with blue screening to mimic approximate *in situ* light

conditions (∼33% light level). Additional samples were collected for T_{zero} $\delta^{15}PN$ natural abundance measurements and for DNA. Incubations were terminated after 12 h and all bottles were subsampled for CARD-FISH and nanoSIMS (see below).

The effect of depth on UCYN-A *nifH* gene expression was examined via nucleic acid collection over a diel cycle. During the period of sampling, the ship was conducting Lagrangian observations near the centre of the cyclonic eddy, which were facilitated by tracking surface velocity program drifters that had drogues centered at 15 and 120 m. Conducting Lagrangian observations within the eddy minimized the potential impact of different water masses and thereby facilitated observations of biological variability over the diel period. Triplicate seawater samples were collected from depths of 5, 75, and 100 m at 07:30, 13:00, 16:00, 19:00, 22:00, 01:30, 03:30, and 07:30 the following day using Niskin® sampling bottles attached to the CTD rosette, and were subsampled into 4.3 l acid-washed, MilliQ-rinsed polycarbonate bottles. DNA and RNA were preserved and extracted from the same sample, complementary DNA (cDNA) was constructed, and UCYN-A1 *nifH* genes in DNA and cDNA were quantified using droplet digital PCR (ddPCR) (see below).

Community NFRs

Community NFRs were measured using the $^{15}N_2$ method of Montoya *et al.* (1996), with modifications to avoid incomplete $^{15}N_2$ bubble dissolution (Mohr *et al.*, 2010). The $^{15}N_2$ tracer was added as $^{15}N_2$-enriched seawater, which was prepared prior to the research cruise using surface seawater from Station ALOHA, as described by Wilson *et al.* (2012). Seawater was filtered using a 0.2 μm in-line filter, then degassed via bubbling with helium gas, vacuuming, heating, and stirring. The degassed seawater was subsequently injected with ∼13 ml $^{15}N_2$ gas (99 atom%, Cambridge Isotope Laboratories, Tewksbury, USA) per litre seawater and manually agitated to facilitate bubble dissolution. This $^{15}N_2$-enriched seawater was dispensed into gas serum bottles which were brought to sea and stored at 4°C prior to use. The $^{15}N/^{14}N$ ratio of each batch of $^{15}N_2$-enriched seawater (five batches total) was measured prior to the cruise via membrane inlet mass spectrometry according to Ferrón *et al.* (2016), yielding $^{15}N_2$ atom% values ranging from 81.3% to 88.5%. These values were used to calculate initial $^{15}N_2$ atom% values for all incubation bottles (2.7%–3.2%). We note that a recent study by White *et al.* (2020) indicates that measuring the $^{15}N_2$ atom% of the enriched seawater rather than the final inoculum may have biased our initial $^{15}N_2$ atom% estimates, leading to

a relatively small (< 20%) overestimation of calculated rates.

For the *in situ* array and deck-board incubation experiments, 4.3 l sampling bottles were filled to capacity with collected seawater, 100 ml of seawater was removed and replaced with an equal volume of $^{15}N_2$-enriched seawater, and bottles were capped. Incubations were terminated via peristaltic pump filtration onto pre-combusted glass fibre filters (GF/F, Whatman, Little Chalfont, United Kingdom). T$_{zero}$ (non-enriched) $\delta^{15}PN$ natural abundance samples were also collected from each sampling depth and immediately filtered at the initiation of each experiment. Filters were frozen at $-80°C$ and transported to the University of Hawaii, Manoa where they were dried overnight at $60°C$ and packaged into tin capsules. Concentrations and isotopic composition ($\delta^{15}N$) of particulate N were analysed via a continuous-flow isotope ratio mass spectrometry using a Carlo-Erba EA NC2500 coupled with Thermo Finnigan DeltaPlus XP at the University of Hawaii Stable Isotope Facility. Rates of $^{15}N_2$ fixation were calculated as described by Montoya *et al*. (1996). Detection limits were calculated by setting the minimal acceptable change in the $\delta^{15}N$ of particulate N through the incubation to 4‰.

UCYN-A cell-specific NFRs

Subsamples of community N$_2$ fixation incubation bottles and T$_{zero}$ (non-enriched) $\delta^{15}PN$ natural abundance samples were preserved in order to measure UCYN-A cell-specific NFRs. 95 ml of seawater was subsampled into amber bottles and fixed with 5 ml of 37%, pre-filtered formaldehyde. Fixed samples were stored for up to 48 h at $4°C$, then were gently vacuum-filtered through 25 mm diameter, 0.6 µm pore-size Isopore polycarbonate filters (EMD Millipore, Hayward, USA) atop 0.8 µm pore-size cellulose acetate backing filters (Sterlitech, Kent, USA). Filters were rinsed with MilliQ water, dried, and stored at $-80°C$.

UCYN-A symbioses were visualized using a double CARD-FISH assay. Details of the CARD-FISH procedure and preparation for nanoSIMS are described in Gradoville *et al*. (2020). This CARD-FISH assay included two separate hybridizations to label UCYN-A (Krupke *et al*., 2013) and the haptophyte host (Cornejo-Castillo *et al*., 2016), without the use of competitor oligonucleotides. After CARD-FISH, cells were transferred to gridded silicon wafers (Pelcotec SFG12 Finder Grid Substrate, Ted Pella, Redding, USA). Intact UCYN-A associations containing fluorescent label for both host and symbiont and with diameters < 3 µm (to target UCYN-A1 and exclude larger UCYN-A sublineages) were identified, imaged, and mapped using a Zeiss Axioplan epifluorescence microscope at UC Santa Cruz.

The isotopic composition of N within UCYN-A symbioses was measured using a Cameca NanoSIMS 50 L at the Stanford Nano Shared Facilities laboratory (http://snsf.stanford.edu). Details for nanoSIMS measurements and data analysis are provided in Gradoville *et al*. (2020). A total of 173 associations were analysed (8–12 associations per sample). The look@nanoSIMS software (Polerecky *et al*., 2012) was used to accumulate plane images and draw regions of interest around UCYN-A associations (both host and symbiont were analysed together as a single association). The $^{15}N/^{14}N$ ratio (calculated as $^{12}C^{15}N/^{12}C^{14}N$) was determined for each region of interest, and diameters were estimated from the perimeter, assuming a spherical shape. An example nanoSIMS image is provided in Fig. S2. NFRs by UCYN-A associations were calculated using the equation of Montoya *et al*. (1996) with a modification to replace the particulate N concentration term with the estimated cellular N content of each symbiosis. Cellular N content estimates are based on the measured diameter of each symbiosis (from look@nanoSIMS output), which was used to calculate cell volume assuming a spherical shape. Cell volume was converted to cellular carbon content based on the equation of Verity *et al*. (1992) and converted to cellular N content using a C:N ratio of 6.3 previously determined for UCYN-A symbioses (Martínez-Pérez *et al*., 2016). The initial atom% term (T$_{initial}$) was measured from 32 analysed unenriched symbioses (0.3809 $\pm$ 0.0066 atom% ^{15}N). Detection limits for cell-specific rates were determined by setting the minimum change in atom% ^{15}N through the incubation period as three times the standard deviation of measured values for these unenriched symbioses.

Note that several different approaches have been applied to calculate single-cell assimilation rates (e.g. Thompson *et al*., 2012; Stryhanyuk *et al*., 2018; Mills *et al*., 2020). Our calculated NFRs may underestimate true cell-specific NFRs, since (i) rates can be underestimated when the atom% values of enriched cells approach $^{15}N_2$ atom% (Stryhanyuk *et al*., 2018), (ii) calculating assimilation rates relative to a final element content can underestimate rates of actively dividing cells (Hryhoriy Stryhanyuk, pers. comm.), (iii) ^{15}N may be diluted through the CARD-FISH procedure (Musat *et al*., 2014; Meyer *et al*., 2020), and (iv) fixed N could be rapidly transferred to other organisms or to dissolved organic or inorganic N pools. Our approach is consistent with previous nanoSIMS-based studies of UCYN-A (Gradoville *et al*., 2020; Mills *et al*., 2020) and includes the atom% T$_{initial}$ term in the denominator of the assimilated fraction; this term is present in the original bulk NFR equation (Montoya *et al*., 1996) but has been omitted in some cell-specific NFR calculations (e.g., Thompson *et al*., 2012). All data used for rate calculations are provided in Table S4.

Nucleic acid extraction, cDNA synthesis, and ddPCR

Different methods were used to preserve and extract nucleic acids from the $^{15}N_2$ incubation and diel sampling experiments. For $^{15}N_2$ experiments (both deck-board incubations and *in situ* arrays), DNA samples were collected onto 0.2 μm pore-size Supor membranes (MilliporeSigma, Burlington, USA). Filters were placed into microcentrifuge tubes containing mixtures of 0.1 and 0.5 mm glass beads (Biospec products, Bartlesville, USA), flash-frozen in liquid N_2, and stored at $-80°C$ until processing. DNA was extracted using the DNeasy Plant Mini Kit with the QIAcube instrument (Qiagen, Venlo, Netherlands), following the manufacturer's protocol with additional steps of three flash freeze/thaw cycles, 2 min of bead-beating, and a Proteinase K treatment, as described by Moisander *et al*. (2010). The final DNA elution volume was 100 μl. Extracts were stored at $-20°C$ prior to ddPCR.

For diel experiment samples, seawater was filtered through 0.2 μm pore-size Sterivex polyethersulfone membranes (MilliporeSigma) with a maximum filtration time of 20 min. Filters were flash-frozen in liquid N_2 and stored at $-80°C$ until extraction. DNA and RNA were extracted simultaneously using the AllPrep DNA/RNA Mini Kit (Qiagen). Extractions used the manufacturer's protocol with the following modifications: three flash freeze/thaw cycles, bead-beating for 2 min, DNase treatment for RNA extracts (RNase-Free DNase Set, Qiagen), and a 60 μl final elution volume. DNA samples were stored at $-20°C$ prior to analysis. Two aliquots of RNA extract were immediately frozen and stored at $-80°C$ to be tested for quality and used as RNA-only controls for ddPCR. RNA quality testing was performed using a Bioanalyzer RNA 6000 Nano assay kit (Agilent, Santa Clara, USA) using the manufacturer's protocol. Immediately following extractions, aliquots of RNA were also used for cDNA synthesis with the Superscript III First-Strand Synthesis System (Thermo Fisher, Waltham, USA) using random hexamer primers.

Digital droplet PCR (ddPCR) was used to quantify the *nifH* genes of nine diazotroph groups. For samples co-located with $^{15}N_2$ incubations, primer/probe sets targeted UCYN-A1 (Church *et al*., 2005a), UCYN-A2/A3 (Thompson *et al*., 2014) *Trichodesmium* (Church *et al*., 2005a), *Crocosphaera* (UCYN-B, Moisander *et al.,* 2010), *Cyanothece*-like organisms (UCYN-C, Foster *et al*., 2007), *Richelia* associated with *Rhizosolenia* (Het-1, Church *et al*., 2005b), *Richelia* associated with *Hemiaulus* (Het-2, Foster *et al*., 2007), *Calothrix* associated with *Chaetoceros* (Het-3, Foster *et al*., 2007), and the gammaproteobacterial group 'Gamma-A' (Moisander *et al*., 2008). For the diel experiment samples, DNA, cDNA, and RNA-only controls were used to quantify UCYN-A1 only.

All ddPCR assays were run in duplicate or triplicate using the ddPCR Supermix for Probes (no dUTP) (Bio-Rad Laboratories, Hercules, USA) with either 6-FAM™ or HEX™ chemistry (Integrated DNA Technologies, Coralville, USA). Final 20 μl reactions (after droplet generation) consisted of 1X Supermix, 0.4 μM forward primer, 0.4 μM reverse primer, 0.2 μM probe, and 1.6 μl DNA (or cDNA or RNA). Droplets were generated using a Bio-Rad Automated Droplet Generator and cycled on a Bio-Rad 1000 Touch™ Thermal Cycler. Reactions were cycled at $95°C$ for 10 min, followed by 40 cycles of $94°C$ for 30 s then $64°C$ for 1 min, and finally $98°C$ for 10 min, with the exception of UCYN-B, UCYN-C, and *Trichodesmium* assays, which used an annealing temperature of $60°C$ rather than $64°C$. The optimal annealing temperature for each assay was empirically tested before running samples. *Trichodesmium* (FAM) and UCYN-C (HEX) assays were run simultaneously in the same wells, as multiplex tests indicated no cross-reactivity between the primers or probes of these assays. The fluorescent signals of amplified droplets were measured using a Bio-Rad QX200 Droplet Reader.

Data were analysed using the QuantaSoft™ Analysis Pro software. Manual thresholds were set to differentiate positive from negative droplets, and samples with < 10 000 droplets were discarded. No template control (NTC) reactions were included on all runs. Detection limits were set as the average plus three times the standard deviation of NTC samples; this was evaluated separately for each assay. For all diel experiment samples, copy numbers detected in RNA-only controls were either below LOD or else at least two orders of magnitude lower than the copy number detected in the corresponding DNA sample.

Biogeochemical and hydrological data

All water-column sampling was conducted using a rosette with a CTD package (SBE 911Plus, SeaBird) that had additional sensors for fluorescence and oxygen. The fluorescence sensor was calibrated for chlorophyll *a* and phaeopigments (chloropigments) using a Turner 10 AU fluorometer (Strickland and Parsons, 1972). Mixed layer depths were calculated using a 0.03 potential density offset relative to the potential density at 10 m (de Boyer Montégut *et al*., 2004). Inorganic nutrient samples were collected using sampling bottles attached to the CTD rosette. Seawater was subsampled into 125 ml high-density polyethylene bottles; these samples were frozen and transported to the University of Hawaii, Manoa where they were analysed for N + N and SRP following Foreman *et al*. (2019).

Surface PAR was measured using a LICOR LI-1500 Light Sensor Logger on the ship's deck. Daily integrated

surface PAR and daily average surface PAR were calculated by summing and averaging surface PAR from daylight hours, respectively. The percentage PAR at each sampling depth was measured using a free-falling optical profiler (Satlantic Hyper-Pro, Sea-Bird Scientific, Bellevue, USA) deployed at noon the day of each experiment. PAR values at each depth were calculated by multiplying daily PAR (integrated or averaged) by the percentage PAR at each depth, using a factor of 1.2 to transform the downwelling planar irradiance to a scalar (downwelling + upwelling) irradiance (Wozniak *et al.*, 2003; Letelier *et al.*, 2017).

Light response curves

Light response curves were fit for UCYN-A using cell-specific NFRs from the *in situ* array experiments and for other cyanobacterial diazotroph taxa using literature values from laboratory studies. When data were only available in graphical form, means were extracted using the program WebPlotDigitizer (Rohatgi, 2020). All curves used the model of Webb *et al.* (1974):

$$NFR = NFR_{max}\left(1 - \exp\left(-\frac{\alpha I}{NFR_{max}}\right)\right) + NFR_0,$$

where NFR_{max} represents maximum NFR, α represents the light affinity coefficient, I represents irradiance (average daily light intensity for *in situ* array experiments), and NFR_0 represents N$_2$ fixation in the dark. Models were fit using the nls function in R (version 4.0.0; http://www.r-project.org/). The light saturation parameter I_k was calculated as NFR_{max}/α. Error for I_k was estimated by propagating the standard errors for NFR_{max} and α given by the nls function.

Statistical analyses

Two-way ANOVA and subsequent Tukey HSD post hoc tests were used to test the effects of depth and eddy polarity (cyclonic vs. anticyclonic) on UCYN-A cell-specific NFRs as well as the effects of time and depth on UCYN-A *nifH* gene-specific transcriptional activity. Tests were performed in R.

Acknowledgements

References

Barone, B., Coenen, A.R., Beckett, S.J., McGillicuddy, D.J., Weitz, J.S., and Karl, D.M. (2019) The ecological and biogeochemical state of the North Pacific Subtropical Gyre is linked to sea surface height. *J Mar Res* **77**: 215–245.

Behrenfeld, M.J., and Falkowski, P.G. (1997) A consumer's guide to phytoplankton primary productivity models. *Limnol Oceanogr* **42**: 1479–1491.

Berman-Frank, I., Lundgren, P., Chen, Y.-B., Küpper, H., Kolber, Z., Bergman, B., and Falkowski, P. (2001) Segregation of nitrogen fixation and oxygenic photosynthesis in the marine cyanobacterium *Trichodesmium*. *Science* **294**: 1534–1537.

Boström, K.H., Simu, K., Hagström, Å., and Riemann, L. (2004) Optimization of DNA extraction for quantitative marine bacterioplankton community analysis. *Limnol Oceanogr Meth* **2**: 365–373.

Böttjer, D., Dore, J.E., Karl, D.M., Letelier, R.M., Mahaffey, C., Wilson, S.T., *et al.* (2017) Temporal variability of nitrogen fixation and particulate nitrogen export at Station ALOHA. *Limnol Oceanogr* **62**: 200–216.

Breitbarth, E., Wohlers, J., Kläs, J., LaRoche, J., and Peeken, I. (2008) Nitrogen fixation and growth rates of *Trichodesmium* IMS-101 as a function of light intensity. *Mar Ecol Prog Ser* **359**: 25–36.

Chen, Y.-B., Dominic, B., Zani, S., Mellon, M.T., and Zehr, J.P. (1999) Expression of photosynthesis genes in relation to nitrogen fixation in the diazotrophic filamentous nonheterocystous cyanobacterium *Trichodesmium* sp. IMS 101. *Plant Mol Biol* **41**: 89–104.

Cheung, S., Nitanai, R., Tsurumoto, C., Endo, H., Nakaoka, S.I., Cheah, W., *et al.* (2020) Physical forcing controls the basin-scale occurrence of nitrogen-fixing organisms in the North Pacific Ocean. *Global Biogeochem Cy* **34**, e2019GB006452.

Church, M.J., Jenkins, B.D., Karl, D.M., and Zehr, J.P. (2005a) Vertical distributions of nitrogen-fixing phylotypes at Stn ALOHA in the oligotrophic North Pacific Ocean. *Aquat Microb Ecol* **38**: 3–14.

Church, M.J., Mahaffey, C., Letelier, R.M., Lukas, R., Zehr, J.P., and Karl, D.M. (2009) Physical forcing of nitrogen fixation and diazotroph community structure in the North Pacific Subtropical Gyre. *Global Biogeochem Cy* **23**: GB2020.

Church, M.J., Short, C.M., Jenkins, B.D., Karl, D.M., and Zehr, J.P. (2005b) Temporal patterns of nitrogenase gene (*nifH*) expression in the oligotrophic North Pacific Ocean. *Appl Environ Microbiol* **71**: 5362–5370.

Cornejo-Castillo, F.M., Cabello, A.M., Salazar, G., Sánchez-Baracaldo, P., Lima-Mendez, G., Hingamp, P., *et al.* (2016) Cyanobacterial symbionts diverged in the late Cretaceous towards lineage-specific nitrogen fixation factories in single-celled phytoplankton. *Nat Commun* **7**: 11071.

Cornejo-Castillo, F.M., and Zehr, J.P. (2019) Hopanoid lipids may facilitate aerobic nitrogen fixation in the ocean. *PNAS USA* **116**: 18269–18271.

de Boyer Montégut, C., Madec, G., Fischer, A.S., Lazar, A., and Iudicone, D. (2004) Mixed layer depth over the global ocean: an examination of profile data and a profile-based climatology. *J Geophys Res Oceans* **109**: C12003.

del Carmen Muñoz-Marin, M., Shilova, I.N., Shi, T., Farnelid, H., Cabello, A.M., and Zehr, J.P. (2019) The transcriptional cycle is suited to daytime N2 fixation in the unicellular cyanobacterium "Candidatus *Atelocyanobacterium thalassa*" (UCYN-A). *MBio* **10**: e02495–e02418.

Falkowski, P.G. (1983) Enzymology of nitrogen assimilation. In *Nitrogen in the Marine Environment*: New York: Elsevier, pp. 839–868.

Ferrón, S., del Valle, D.A., Björkman, K.M., Quay, P.D., Church, M.J., and Karl, D.M. (2016) Application of membrane inlet mass spectrometry to measure aquatic gross primary production by the ^{18}O *in vitro* method. *Limnol Oceanogr Meth* **14**: 610–622.

Fong, A.A., Karl, D.M., Lukas, R., Letelier, R.M., Zehr, J.P., and Church, M.J. (2008) Nitrogen fixation in an anticyclonic eddy in the oligotrophic North Pacific Ocean. *ISME J* **2**: 663–676.

Foreman, R.K., Björkman, K.M., Carlson, C.A., Opalk, K., and Karl, D.M. (2019) Improved ultraviolet photo-oxidation system yields estimates for deep-sea dissolved organic nitrogen and phosphorus. *Limnol Oceanogr Meth* **17**: 277–291.

Forget, M.-H., Sathyendranath, S., Platt, T., Pommier, J., Vis, C., Kyewalyanga, M., and Hudon, C. (2007) Extraction of photosynthesis-irradiance parameters from phytoplankton production data: demonstration in various aquatic systems. *J Plankton Res* **29**: 249–262.

Foster, R., Subramaniam, A., Mahaffey, C., Carpenter, E., Capone, D., and Zehr, J. (2007) Influence of the Amazon River plume on distributions of free-living and symbiotic cyanobacteria in the western tropical North Atlantic Ocean. *Limnol Oceanogr* **52**: 517–532.

Foster, R.A., Goebel, N.L., and Zehr, J.P. (2010) Isolation of *Calothrix rhizosoleniae* (cyanobacteria) strain SC01 from *Chaetoceros* (Bacillariophyta) spp. diatoms of the subropical North Pacific Ocean. *J Phycol* **46**: 1028–1037.

Gallon, J. (1992) Tansley review no. 44. Reconciling the incompatible: N2 fixation and O2. *New Phytol* **122**: 571–609.

Galloway, J.N., Dentener, F.J., Capone, D.G., Boyer, E.W., Howarth, R.W., Seitzinger, S.P., *et al*. (2004) Nitrogen cycles: past, present, and future. *Biogeochemistry* **70**: 153–226.

Garcia, N.S., Fu, F.-X., and Hutchins, D.A. (2013) Colimitation of the unicellular photosynthetic diazotroph *Crocosphaera watsonii* by phosphorus, light, and carbon dioxide. *Limnol Oceanogr* **58**: 1501–1512.

Goebel, N.L., Edwards, C.A., Carter, B.J., Achilles, K.M., and Zehr, J.P. (2008) Growth and carbon content of three different-sized diazotrophic cyanobacteria observed in the Subtropical North Pacific. *J Phycol* **44**: 1212–1220.

Gradoville, M.R., Bombar, D., Crump, B.C., Letelier, R.M., Zehr, J.P., and White, A.E. (2017) Diversity and activity of nitrogen-fixing communities across ocean basins. *Limnol Oceanogr* **62**: 1895–1909.

Gradoville, M.R., Farnelid, H., White, A.E., Turk-Kubo, K.A., Stewart, B., Ribalet, F., *et al*. (2020) Latitudinal constraints

on the abundance and activity of the cyanobacterium UCYN-A and other marine diazotrophs in the North Pacific. *Limnol Oceanogr* **65**: 1858–1875.

Harding, K., Turk-Kubo, K.A., Sipler, R.E., Mills, M.M., Bronk, D.A., and Zehr, J.P. (2018) Symbiotic unicellular cyanobacteria fix nitrogen in the Arctic Ocean. *PNAS USA* **115**: 13371–13375.

Jayakumar, A., Al-Rshaidat, M., Ward, B.B., and Mulholland, M. R. (2012) Diversity, distribution, and expression of diazotroph nifH genes in oxygen-deficient waters of the Arabian Sea. *FEMS Microbiol Ecol* **82**: 597–606.

Karl, D., Letelier, R., Tupas, L., Dore, J., Christian, J., and Hebel, D. (1997) The role of nitrogen fixation in biogeochemical cycling in the subtropical North Pacific Ocean. *Nature* **388**: 533–538.

Kovač, Ž., Platt, T., Sathyendranath, S., and Morović, M. (2016a) Analytical solution for the vertical profile of daily production in the ocean. *J Geophys Res Oceans* **121**: 3532–3548.

Kovač, Ž., Platt, T., Sathyendranath, S., Morović, M., and Jackson, T. (2016b) Recovery of photosynthesis parameters from in situ profiles of phytoplankton production. *ICES J Mar Sci* **73**: 275–285.

Kranz, S.A., Levitan, O., Richter, K.U., Prášil, O., Berman-Frank, I., and Rost, B. (2010) Combined effects of CO_2 and light on the N2-fixing cyanobacterium *Trichodesmium* IMS101: physiological responses. *Plant Physiol* **154**: 334–345.

Krupke, A., Mohr, W., LaRoche, J., Fuchs, B.M., Amann, R. I., and Kuypers, M.M. (2015) The effect of nutrients on carbon and nitrogen fixation by the UCYN-A–haptophyte symbiosis. *ISME J* **9**: 1635–1647.

Krupke, A., Musat, N., LaRoche, J., Mohr, W., Fuchs, B.M., Amann, R.I., *et al*. (2013) *In situ* identification and N2 and C fixation rates of uncultivated cyanobacteria populations. *Syst Appl Microbiol* **36**: 259–271.

Letelier, R., Dore, J., Winn, C., and Karl, D. (1996) Seasonal and interannual variations in photosynthetic carbon assimilation at station. *Deep Sea Res Part II Top Stud Oceanogr* **43**: 467–490.

Letelier, R.M., Karl, D.M., Abbott, M.R., and Bidigare, R.R. (2004) Light driven seasonal patterns of chlorophyll and nitrate in the lower euphotic zone of the North Pacific Subtropical Gyre. *Limnol Oceanogr* **49**: 508–519.

Letelier, R.M., White, A.E., Bidigare, R.R., Barone, B., Church, M.J., and Karl, D.M. (2017) Light absorption by phytoplankton in the North Pacific Subtropical Gyre. *Limnol Oceanogr* **62**: 1526–1540.

Levitan, O., Kranz, S.A., Spungin, D., Prášil, O., Rost, B., and Berman-Frank, I. (2010) Combined effects of CO_2 and light on the N2-fixing cyanobacterium *Trichodesmium* IMS101: a mechanistic view. *Plant Physiol* **154**: 346–356.

Li, B., Karl, D.M., Letelier, R.M., and Church, M.J. (2011) Size-dependent photosynthetic variability in the North Pacific Subtropical Gyre. *Mar Ecol Prog Ser* **440**: 27–40.

Luo, Y.-W., Lima, I., Karl, D., Deutsch, C., and Doney, S. (2014) Data-based assessment of environmental controls on global marine nitrogen fixation. *Biogeosciences* **11**: 691–708.

Martínez-Pérez, C., Mohr, W., Löscher, C.R., Dekaezemacker, J., Littmann, S., Yilmaz, P., *et al*. (2016)

The small unicellular diazotrophic symbiont, UCYN-A, is a key player in the marine nitrogen cycle. *Nat Microbiology* **1**: 16163.

McGillicuddy, D., and Robinson, A. (1997) Eddy-induced nutrient supply and new production in the Sargasso Sea. *Deep Sea Res Part I Oceanogr Res Pap* **44**: 1427–1450.

Meyer, N.R., Fortney, J., and Dekas, A.E. (2020) NanoSIMS sample preparation decreases isotope enrichment: magnitude, variability and implications for single-cell rates of microbial activity. *Environ Microbiol* **23**: 81–98. https://doi.org/10.1111/1462-2920.15264.

Milligan, A.J., Berman-Frank, I., Gerchman, Y., Dismukes, G.C., and Falkowski, P.G. (2007) Light-dependent oxygen consumption in nitrogen-fixing cyanobacteria plays a key role in nitrogenase protection. *J Phycol* **43**: 845–852.

Mills, M.M., Turk-Kubo, K.A., van Dijken, G.L., Henke, B.A., Harding, K., Wilson, S.T., et al. (2020) Unusual marine cyanobacteria/haptophyte symbiosis relies on N₂ fixation even in N-rich environments. *ISME J* **14**: 2395–2406.

Mitsui, A., Kumazawa, S., Takahashi, A., Ikemoto, H., Cao, S., and Arai, T. (1986) Strategy by which nitrogen-fixing unicellular cyanobacteria grow photoautotrophically. *Nature* **323**: 720–722.

Mohr, W., Großkopf, T., Wallace, D.W.R., and LaRoche, J. (2010) Methodological underestimation of oceanic nitrogen fixation rates. *PLoS One* **5**: e12583.

Moisander, P.H., Beinart, R.A., Hewson, I., White, A.E., Johnson, K.S., Carlson, C.A., et al. (2010) Unicellular cyanobacterial distributions broaden the oceanic N₂ fixation domain. *Science* **327**: 1512–1514.

Moisander, P.H., Beinart, R.A., Voss, M., and Zehr, J.P. (2008) Diversity and abundance of diazotrophic microorganisms in the South China Sea during intermonsoon. *ISME J* **2**: 954–967.

Montoya, J.P., Voss, M., Kahler, P., and Capone, D.G. (1996) A simple, high-precision, high-sensitivity tracer assay for N₂ fixation. *Appl Environ Microbiol* **62**: 986–993.

Moore, C., Mills, M., Arrigo, K., Berman-Frank, I., Bopp, L., Boyd, P., et al. (2013) Processes and patterns of oceanic nutrient limitation. *Nat Geosci* **6**: 701–710.

Musat, N., Stryhanyuk, H., Bombach, P., Adrian, L., Audinot, J.-N., and Richnow, H.H. (2014) The effect of FISH and CARD-FISH on the isotopic composition of ¹³C- and ¹⁵N-labeled *Pseudomonas putida* cells measured by nanoSIMS. *Syst Appl Microbiol* **37**: 267–276.

Ohki, K., Zehr, J.P., and Fujita, Y. (1992) Regulation of nitrogenase activity in relation to the light-dark regime in the filamentous non-heterocystous cyanobacterium *Trichodesmium* sp. NIBB 1067. *Microbiology* **138**: 2679–2685.

Polerecky, L., Adam, B., Milucka, J., Musat, N., Vagner, T., and Kuypers, M.M. (2012) Look@ NanoSIMS–a tool for the analysis of nanoSIMS data in environmental microbiology. *Environ Microbiol* **14**: 1009–1023.

Raes, E.J., van de Kamp, J., Bodrossy, L., Fong, A.A., Riekenberg, J., Holmes, B.H., et al. (2020) N₂ fixation and new insights into nitrification from the ice-edge to the equator in the South Pacific Ocean. *Front Mar Sci* **7**: 389.

Richardson, K., Beardall, J., and Raven, J. (1983) Adaptation of unicellular algae to irradiance: an analysis of strategies. *New Phytol* **93**: 157–191.

Rohatgi, A. (2020). WebPlotDigitizer v4.3. URL https://automeris.io/WebPlotDigitizer.

Sargent, E.C., Hitchcock, A., Johansson, S.A., Langlois, R., Moore, C.M., LaRoche, J., et al. (2016) Evidence for polyploidy in the globally important diazotroph *Trichodesmium*. *FEMS Microbiol Lett* **363**: fnw244.

Shiozaki, T., Bombar, D., Riemann, L., Hashihama, F., Takeda, S., Yamaguchi, T., et al. (2017) Basin scale variability of active diazotrophs and nitrogen fixation in the North Pacific, from the tropics to the subarctic Bering Sea. *Global Biogeochem Cycles* **31**: 996–1009.

Staal, M., te Lintel Hekkert, S., Herman, P., and Stal, L.J. (2002) Comparison of models describing light dependence of N₂ fixation in heterocystous cyanobacteria. *Appl Environ Microbiol* **68**: 4679–4683.

Strickland, J., and Parsons, T. (1972) *A Practical Handbook of Seawater Analysis*. Ottawa, ON: Fisheries Research Board of Canada.

Stryhanyuk, H., Calabrese, F., Kümmel, S., Musat, F., Richnow, H.H., and Musat, N. (2018) Calculation of single cell assimilation rates from SIP-NanoSIMS-derived isotope ratios: a comprehensive approach. *Front Microbiol* **9**: 2342.

Tang, W., and Cassar, N. (2019) Data-driven modeling of the distribution of diazotrophs in the global ocean. *Geophys Res Lett* **46**: 12258–12269.

Thompson, A., Carter, B.J., Turk-Kubo, K., Malfatti, F., Azam, F., and Zehr, J.P. (2014) Genetic diversity of the unicellular nitrogen-fixing cyanobacteria UCYN-A and its prymnesiophyte host. *Environ Microbiol* **16**: 3238–3249.

Thompson, A.W., Foster, R.A., Krupke, A., Carter, B.J., Musat, N., Vaulot, D., et al. (2012) Unicellular cyanobacterium symbiotic with a single-celled eukaryotic alga. *Science* **337**: 1546–1550.

Tripp, H.J., Bench, S.R., Turk, K.A., Foster, R.A., Desany, B.A., Niazi, F., et al. (2010) Metabolic streamlining in an open-ocean nitrogen-fixing cyanobacterium. *Nature* **464**: 90–94.

Tuit, C., Waterbury, J., and Ravizza, G. (2004) Diel variation of molybdenum and iron in marine diazotrophic cyanobacteria. *Limnol Oceanogr* **49**: 978–990.

Turk-Kubo, K.A., Achilles, K.M., Serros, T.R., Ochiai, M., Montoya, J.P., and Zehr, J.P. (2012) Nitrogenase (*nifH*) gene expression in diazotrophic cyanobacteria in the tropical North Atlantic in response to nutrient amendments. *Front Microbiol* **3**: 386.

Turk-Kubo, K.A., Farnelid, H.M., Shilova, I.N., Henke, B., and Zehr, J.P. (2017) Distinct ecological niches of marine symbiotic N₂-fixing cyanobacterium *Candidatus Atelocyanobacterium thalassa* sublineages. *J Phycol* **53**: 451–461.

Verity, P.G., Robertson, C.Y., Tronzo, C.R., Andrews, M.G., Nelson, J.R., and Sieracki, M.E. (1992) Relationships between cell volume and the carbon and nitrogen content of marine photosynthetic nanoplankton. *Limnol Oceanogr* **37**: 1434–1446.

Villareal, T. (1992) Marine nitrogen-fixing diatom-cyanobacteria symbioses. In *Marine Pelagic Cyanobacteria: Trichodesmium and Other Diazotrophs*, Carpenter, E.J., Capone, D.G., and Rueter, J.G. (eds). Dordrecht, Netherlands: Kluwer, pp. 163–175.

Villareal, T.A. (1990) Laboratory culture and preliminary characterization of the nitrogen-fixing *Rhizosolenia-Richelia* symbiosis. *Mar Ecol* **11**: 117–132.

Vislova, A., Sosa, O.A., Eppley, J., Romano, A., and DeLong, E.F. (2019) Diel oscillation of microbial gene transcription declines with increasing depth in oligotrophic ocean waters. *Front Microbiol* **10**: 2191.

Wang, W.-L., Moore, J.K., Martiny, A.C., and Primeau, F.W. (2019) Convergent estimates of marine nitrogen fixation. *Nature* **566**: 205–211.

Webb, W.L., Newton, M., and Starr, D. (1974) Carbon dioxide exchange of *Alnus rubra*. *Oecologia* **17**: 281–291.

White, A.E., Granger, J., Selden, C., Gradoville, M.R., Potts, L., Bourbonnais, A., *et al*. (2020) A critical review of the $^{15}N_2$ tracer method to measure diazotrophic production in pelagic ecosystems. *Limnol Oceanogr Meth* **18**: 129–147.

Williams, P.J.l.B., Morris, P.J., and Karl, D.M. (2004) Net community production and metabolic balance at the oligotrophic ocean site, station ALOHA. *Deep Sea Res Part I Oceanogr Res Pap* **51**: 1563–1578.

Wilson, S.T., Aylward, F.O., Ribalet, F., Barone, B., Casey, J.R., Connell, P.E., *et al*. (2017) Coordinated regulation of growth, activity and transcription in natural populations of the unicellular nitrogen-fixing cyanobacterium *Crocosphaera*. *Nat Microbiol* **2**: 17118.

Wilson, S.T., Böttjer, D., Church, M.J., and Karl, D.M. (2012) Comparative assessment of nitrogen fixation methodologies, conducted in the oligotrophic North Pacific Ocean. *Appl Environ Microbiol* **78**: 6516–6523.

Wozniak, B., Dera, J., Ficek, D., Majchrowski, R., Ostrowska, M., and Kaczmarek, S. (2003) Modelling light and photosynthesis in the marine environment. *Oceanologia* **45**: 171–245.

Wyman, M., Zehr, J.P., and Capone, D.G. (1996) Temporal variability in nitrogenase gene expression in natural populations of the marine cyanobacterium *Trichodesmium thiebautii*. *Appl Environ Microbiol* **62**: 1073–1075.

Yang, X., Liu, L., Yin, Z., Wang, X., Wang, S., and Ye, Z. (2020) Quantifying photosynthetic performance of phytoplankton based on photosynthesis–irradiance response models. *Environ Sci Eur* **32**: 1–13.

Zehr, J.P., Bench, S.R., Carter, B.J., Hewson, I., Niazi, F., Shi, T., *et al*. (2008) Globally distributed uncultivated oceanic N_2-fixing cyanobacteria lack oxygenic photosystem II. *Science* **322**: 1110–1112.

Zehr, J.P., and Capone, D.G. (2020) Changing perspectives in marine nitrogen fixation. *Science* **368**: eaay9514.

Zehr, J.P., Montoya, J.P., Jenkins, B.D., Hewson, I., Mondragon, E., Short, C.M., *et al*. (2007) Experiments linking nitrogenase gene expression to nitrogen fixation in the North Pacific Subtropical Gyre. *Limnol Oceanogr* **52**: 169–183.

Zehr, J.P., Shilova, I.N., Farnelid, H.M., del Carmen Muñoz-Marín, M., and Turk-Kubo, K.A. (2016) Unusual marine unicellular symbiosis with the nitrogen-fixing cyanobacterium UCYN-A. *Nat Microbiol* **2**: 16214.

Zehr, J.P., Wyman, M., Miller, V., Duguay, L., and Capone, D.G. (1993) Modification of the Fe protein of nitrogenase in natural populations of *Trichodesmium thiebautii*. *Appl Environ Microbiol* **59**: 669–676.

Zondervan, I. (2007) The effects of light, macronutrients, trace metals and CO_2 on the production of calcium carbonate and organic carbon in coccolithophores—a review. *Deep Sea Res Part II Top Stud Oceanogr* **54**: 521–537.

Supporting Information

Additional Supporting Information may be found in the online version of this article at the publisher's web-site:

Appendix S1: Supplementary Information